

well over a decade later. The Rossby wave generated by the 1982–83 El Niño exists today in the northwest corner of the Pacific Ocean.

Additional evidence for this wave is given by a positive dynamic height anomaly observed in hydrographic data south of Japan at 137° E (ref. 14). This anomaly moves from 18° N in 1984 to almost 30° N in 1989, which agrees well with the movement of the Rossby wave in Figs 3 and 4. Thus, the Rossby wave propagating from North America to the Kuroshio Extension is observed in both the model and the ocean. Two additional ocean model simulations were performed to help isolate the decadal effects of the 1982–83 El Niño. One simulation was initialized in 1984 after the El Niño, and shows the absence of the El Niño-generated Rossby wave at 30° N (Fig. 4c). The other simulation starts in 1981, includes the 1982–83 El Niño, but the wind forcing reverts to an average annual forcing in 1984 to exclude subsequent wind-forced anomalies. It shows the Rossby wave (Fig. 4d), and because no knowledge of actual events in the atmosphere after 1984 was used, it demonstrates the potential for decadal predictions of El Niño-generated Rossby waves and their effects.

In the model, the Rossby wave produces a significant geostrophic velocity anomaly of $\sim 10 \text{ cm s}^{-1}$ in the upper ocean as the wave passes through the Kuroshio Extension in 1991. The geostrophic flow induced by the trailing edge of the Rossby wave reduces the flow of the Kuroshio Extension along 35° N. The leading edge of the Rossby wave induces an eastward velocity perturbation near 40° N. The result is a re-routing of a portion of the Kuroshio Extension transport to $\sim 40^\circ \text{ N}$ during 1991 and subsequent years. During 1991 the largest SST anomalies are found north of the Kuroshio Extension coincident with the maximum Rossby wave effects on the current. These anomalies reach a peak of $>1^\circ \text{ C}$ above mean values observed at other times. After the Rossby wave propagates to the northwest, the geostrophic perturbations on the Kuroshio Extension abate; the extension returns to its normally observed latitude, and the anomalous SSTs begin to disappear.

Corroboration of these events is provided by satellite infrared frontal analyses (J. Szezechowski, unpublished results), which indicate a northward displacement of the Kuroshio Extension in 1990–91 and a southward displacement from 1991 to 1993. In 1992–93, the Rossby wave forms a ridge of high SSH from Japan to Alaska (Fig. 3c). The results presented here indicate that the events giving rise to the trans-Pacific SSH ridge and SST anomaly in 1991–92 originated with the 1982–83 El Niño. Thus the oceanographic effects of a major El Niño have extra-tropical and decadal components.

Climatological effects associated with warm, tropical SST anomalies during major El Niño events are well-documented¹⁵. Surprisingly, the SST anomalies that we observe at much higher latitudes across the North Pacific are of the same amplitude and temporal-spatial extent as those observed in the tropics during major El Niño events. At higher latitudes, significant statistical relationships between SST anomalies in the Pacific Ocean and weather patterns over the North American continent have been found¹⁶. Thus it is possible that the 1982–83 El Niño still has important effects on the climate in 1993. Stated succinctly, the 1982–83 El Niño is not over: its effects have moved from South America to the northwest across the Pacific basin. This Rossby wave should continue to propagate across the far northwest corner of the North Pacific basin for at least another decade, and continue to affect the circulation of the North Pacific.

The deterministic nature of the processes that we report indicates that the ocean is not wholly chaotic and unpredictable, even over basin and decadal scales. Relatively simple planetary wave dynamics, the numerical models that include them, and global satellite data sets provide the necessary tools for long-term oceanic predictions (Fig. 4). Finally, we note that these long-timescale events imply that attempts to determine the climatological or average state of the oceans (a major component

of Earth's climate) will require monitoring of the ocean circulation over decadal timescales. This is indeed a major task which will require synergistic use of numerical ocean models and continuous satellite monitoring for a complete understanding. □

Received 17 January; accepted 9 June 1994.

1. Cane, M. A. *Science* **16**, 1189–1194 (1983).
2. Barber, R. T. & Chavez, F. P. *Science* **16**, 1203–1208 (1983).
3. Barber, R. T. & Chavez, F. P. *Nature* **319**, 279–285 (1983).
4. Rasmusson, E. M. & Wallace, J. M. *Science* **16**, 1195–1202 (1983).
5. Folland, C. K. & Owen, J. A. in *Rep. of a Workshop at the European Centre for Medium-Range Weather Forecasting* 102–114 (Publ. No. 254, WMO, Geneva, Switzerland, 1988).
6. Born, G. H., Mitchell, J. L. & Heyler, G. A. *J. astr. Sci.* **35**, 119–134 (1987).
7. Reynolds, R. W. & Marsico, D. C. *J. Clim.* **6**, 768–774 (1993).
8. Hurlburt, H. E., Walcraft, A. J., Sirkes, Z. & Metzger, E. J. *Oceanography* **5**, 9–18 (1992).
9. Wyrtki, K. J. *phys. Oceanogr.* **5**, 572–584 (1975).
10. Gill, A. E. *Atmosphere-Ocean Dynamics* (Academic, Cambridge, UK, 1982).
11. Johnson, M. A. & O'Brien, J. J. *J. geophys. Res.* **95**, 7155–7166 (1990).
12. White, W. B. & Saur, J. F. T. *J. phys. Oceanogr.* **13**, 531–544 (1983).
13. Jacobs, G. A., Emery, W. J. & Born, G. H. *J. phys. Oceanogr.* **23**, 1155–1175 (1991).
14. Qiu, B. & Joyce, T. M. *J. phys. Oceanogr.* **9**, 1062–1079 (1992).
15. Giantz, M. H., Katz, R. W. & Nicholis, N. *Teleconnections Linking Worldwide Climate Anomalies* (Cambridge Univ. Press, 1991).
16. Barnett, T. P. & Preisendorfer, R. *Mon. Weath. Rev.* **115**, 1825–1850 (1987).
17. Teague, W. J., Carron, M. J. & Hogan, P. J. *J. geophys. Res.* **95**, 7167–7183 (1990).
18. Hurlburt, H. E. & Thompson, J. D. *J. phys. Oceanogr.* **10**, 1611–1651 (1980).
19. Walcraft, A. J. *NOARL Report No. 35* (Naval Research Lab, Stennis Space Center, 1991).
20. Metzger, E. J., Hurlburt, H. E., Kindle, J. C., Sirkes, Z. & Pringle, J. M. *Mar. Technol. Soc. J.* **26**, 23–32 (1992).
21. Hellerman, S. & Rosenstein, M. *J. phys. Oceanogr.* **13**, 1093–1104 (1983).
22. McCreary, J. J. *J. phys. Oceanogr.* **6**, 632–645 (1976).
23. Hurlburt, H. E., Kindle, J. C. & O'Brien, J. J. *J. phys. Oceanogr.* **6**, 621–631 (1976).
24. Kindle, J. C. & Phoebus, P. A. *J. Geophys. Res.* (in the press).
25. Chelton, D. B. & Davis, R. E. *J. phys. Oceanogr.* **12**, 757–784 (1982).

ACKNOWLEDGEMENTS. This work was supported by the US Office of Naval Research and the US Advanced Research Projects Agency.

A unique multitoothed ornithomimosaur dinosaur from the Lower Cretaceous of Spain

Bernardino P. Pérez-Moreno*, José Luis Sanz, Angela D. Buscalloni, José J. Moratalla, Francisco Ortega & Diego Rasskin-Gutman

Unidad de Paleontología, Departamento de Biología, Facultad de Ciencias, Universidad Autónoma de Madrid, 28049-Madrid, Spain

THE Lower Cretaceous lithographic limestones from Las Hoyas (province of Cuenca, Spain) have yielded important vertebrate fossil remains. We report here a new specimen, the first ornithomimosaur theropod found in Europe. *Pelecanimimus polyodon* gen. et sp. nov., has some striking elements preserved, such as the hyoid, sternum and integumentary impressions. The fossil has revealed other unexpected features, including a derived hand in an ancient ornithomimosaur, and a large number of teeth (over 200) with a distinctive morphology. This specimen suggests an alternative evolutionary process towards the toothless condition in Ornithomimosauria, which could be explained by an exaptation. *Pelecanimimus polyodon* stresses the relationship between Troodontidae and Ornithomimosauria.

The Las Hoyas fossil site is one of the most important conservative *lagerstätten* from the Lower Cretaceous of western Europe. It has yielded thousands of specimens including two of the most primitive birds ever found: *Iberomesornis romerali*^{1,2} and *Concornis lacustris*³. A diversified flora and fauna from a lacustrine environment have also been discovered in these lithographic limestones⁴. Non-avian dinosaur remains have not previously been found in Las Hoyas limestones, although some sauropod and *Iguanodon* bones were discovered in equivalent strata of

nearby locations⁵. But in July 1993 remains belonging to a non-avian theropod were discovered.

Theropoda
Tetanurae
Ornithomimosauria
Pelecanimimus polyodon, gen. et sp. nov.

Etymology. *Pelecanus* (Latin), pelican; and *mimus* (Greek), mimic; because of the very long facial part of the skull and the integumentary impressions below the skull, which resemble the gular pouch in the pelican. *Polys* (Greek), many; and *odus* (Greek), teeth; because of its large number of teeth.

Holotype. LH 7777 (Museo de Cuenca, Cuenca, Spain; provisionally housed in the Unidad de Paleontología of the Universidad Autónoma de Madrid, Spain). Articulated anterior half of the skeleton, including skull, complete cervical and almost complete dorsal vertebral series, ribs, pectoral girdle, sternum, right forelimb and nearly complete left forelimb (Fig. 1).

Horizon and locality. Las Hoyas fossil site, Cuenca Province, Spain. Calizas de La Huérguina Formation, Upper Hauterivian–Lower Barremian (Lower Cretaceous)⁶.

Diagnosis. Small ornithomimosaur (2–2.5 m long). Skull with long and shallow snout (maximum length about 4.5 times the maximum height). About 220 teeth: 7 premaxillary, about 30 maxillary and about 75 in the dentary. Heterodont. Maxillary teeth larger than dentary teeth. Teeth unserrated, with a constric-

tion between the crown and the root. There are no complete interdental plates. The maxilla has teeth only in its anterior third, and a sharp edge in the posterior zone. The rostral half of the lower jaw has a straight ventral edge. Ulna and radius are tightly adhered distally. Metacarpal ratio is 0.81:1:0.98.

The skull (Fig. 2a) is nearly complete although the braincase bones are badly crushed. Therefore, the present description is of the external cranial bones from the left half of the skull.

The snout is long and shallow, very similar to *Gallimimus*⁷. As is usual in Ornithomimosauria the premaxilla has a long posteroventral process which has broad contact with the nasal, isolating the maxilla from the external naris. The maxilla presents a long antorbital fossa, which includes one accessory fenestra. The jugal has a long anterior process which contributes to the antorbital fenestra; but the jugal does not reach its rostral border, unlike *Dromiceiomimus*⁸. The dorsal part of the lachrymal forms a small prominence over the level of the prefrontal, which resembles that of *Allosaurus*⁹, but is unlike other ornithomimosaur (although a nasal horn in *Garudimimus* has been reported¹⁰).

The dentition is one of the most striking features of *Pelecanimimus*. Teeth have been previously reported only in *Harpymimus*¹¹, in which 10–12 dentary teeth are present. In *Pelecanimimus* the premaxilla has 7 teeth, the maxilla about 30 and the dentary about 75. It thus has a total of about 220 teeth, the highest tooth count within Theropoda. Unlike any other

FIG. 1 *Pelecanimimus polyodon*. Scale in cm. a, Induced fluorescence ultraviolet light photography. b, Normal light photography. Both pictures were taken before preparation. The slabs that contain the skull and the right hand have been prepared with formic acid after embedding each one in a frame of transparent polyester resin¹⁹ (Fig. 2). The slab that holds the caudal part of the neck, the dorsal vertebrae and the pectoral girdles and humeri is currently being prepared, although some significant features of these bones are reported (see text). c, Coracoids; ha, right hand (see Fig. 2b); hy, hyoid; in, integumentary impressions; lf, left forearm; lh, left humerus; ne, neck; rf, right forearm; rh, right humerus; sc, scapular blade; sk, skull (see Fig. 2a); st, sternum.

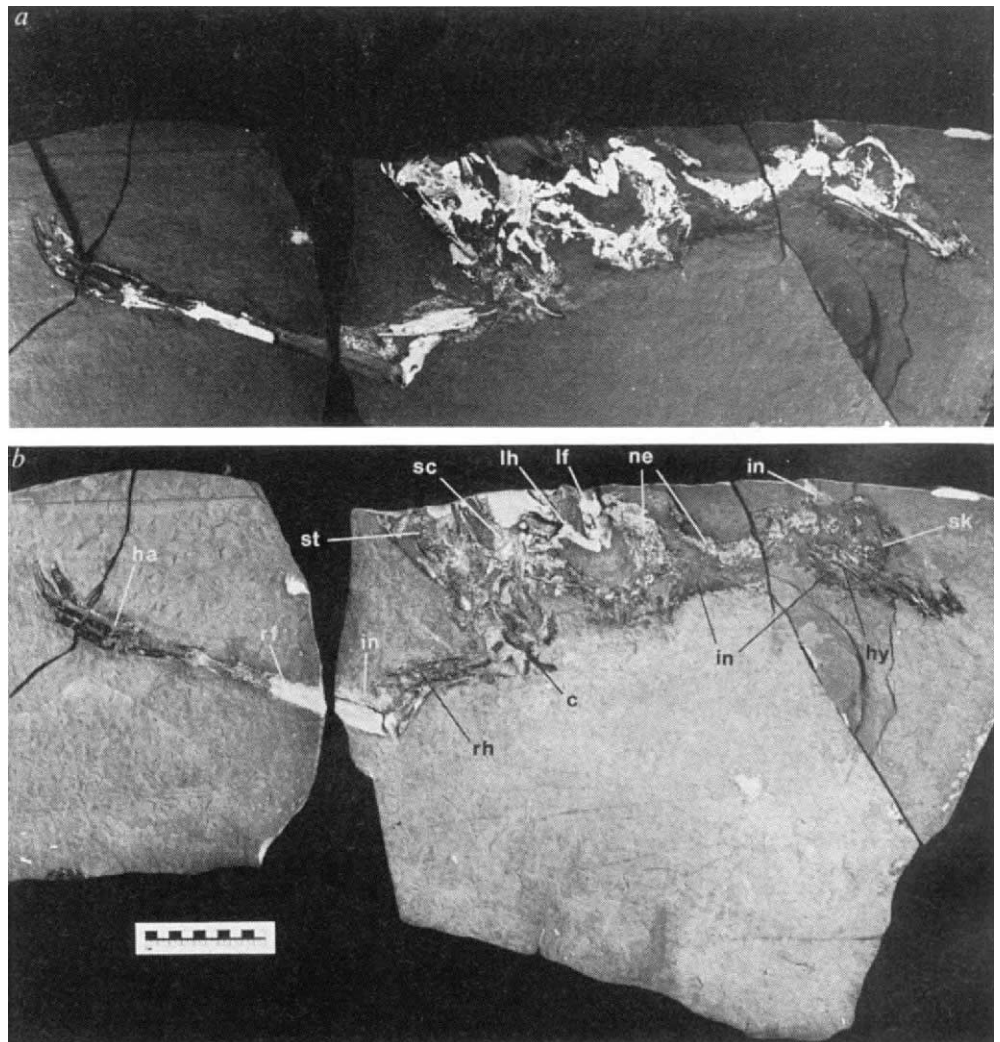
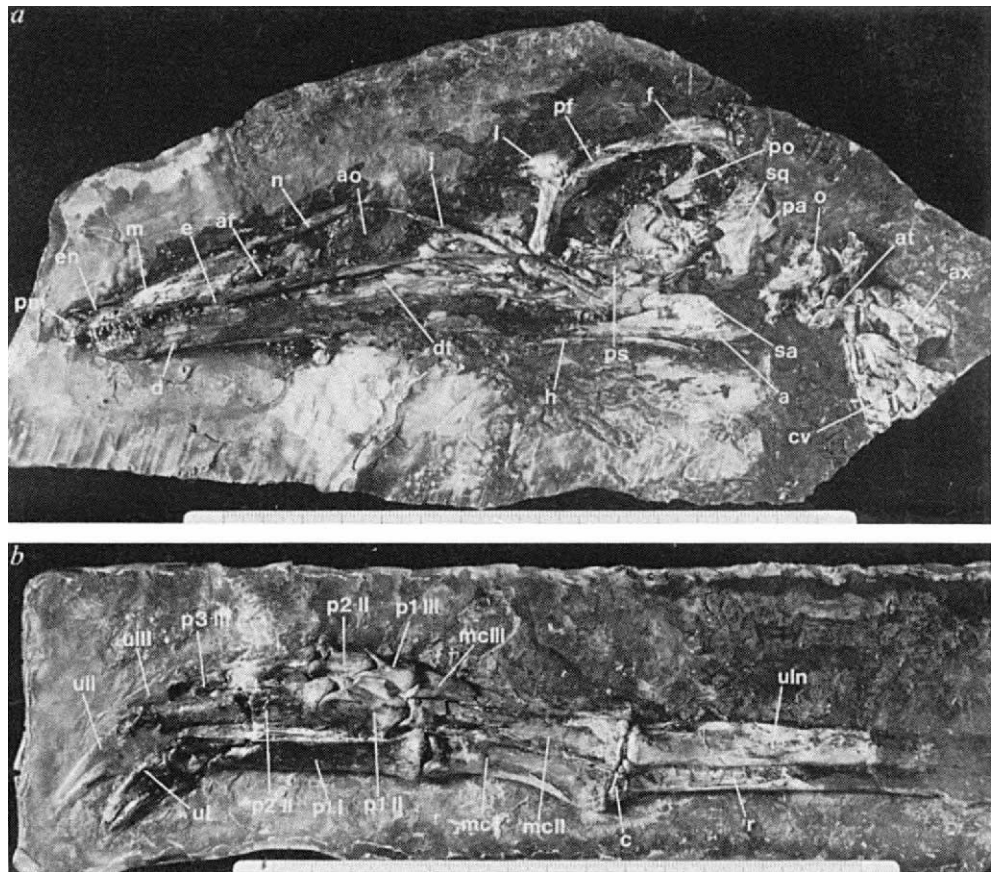


FIG. 2 *Pelecanimimus polyodon*. Scale in mm. **a**, Left side of the skull, atlas, axis and incomplete third cervical vertebra. The facial half of the skull is almost perfectly preserved, but the posterior half is badly crushed. The occipital part of the skull is disconnected from the rest. Therefore, until the counterslab is prepared to allow for a detailed comparison, the identification of some of the bones of this zone remains tentative. **a**, Angular; **af**, accessory fenestra; **ao**, antorbital fenestra; **at**, atlas; **ax**, axis; **cv**, third cervical vertebra; **d**, dentary; **dt**, dentary tooth (the most posterior is marked); **e**, sharp edge of the maxilla; **en**, external naris; **f**, frontal; **h**, hyoid; **j**, jugal; **m**, maxilla; **n**, nasal; **o**, occipital part of the skull; **pa**, parietal; **pf**, prefrontal; **pm**, premaxilla; **po**, postorbital; **ps**, bulbous parasphenoid capsule; **sa**, surangular; **sq**, squamosal. **b**, Extensor side of the right hand and distal part of the forearm. The unguals of the second and third digits and parts of the Mc III are preserved in the counterslab, although they have been copied by the polyester resin in the slab shown. The proximal zone of the forearm (ulna and radius) has been dissolved, but has also been copied by the resin. **c**, Carpals; **mcl**, first metacarpal; **mcll**, second metacarpal; **mclll**, third metacarpal; **p1-I**, first phalanx of first digit; **p1-II**, first phalanx of second digit; **p2-II**, second phalanx of second digit; **p1-III**, first phalanx of the third digit; **p2-III**, second phalanx of third digit; **p3-III**, third phalanx of third digit; **r**, radius; **uln**, ulna; **ul**, ungual of the first digit; **ull**, ungual of the second digit; **ulll**, ungual of the third digit.



theropod, the maxillary teeth are located only in the anterior third of the maxilla, with a sharp edge in the posterior zone. Also surprising is the morphology of the teeth, which are similar to those of Troodontidae¹² (including *Sinornithoides*¹³, from the Lower Cretaceous of China): the teeth have a basal constriction in the crown, and there are no interdental plates. Unlike troodontids, the teeth are unserrated. The anterior teeth have enamel; a more detailed analysis of the posterior ones will be necessary. The premaxillary tooth crowns are incisiform and D-shaped in cross-section. The anterior maxillary teeth are similar to the premaxillary ones, and they gradually become blade-like towards the posterior zone, with mesial and distal carinae. The dentary teeth are clearly smaller than those of the upper jaw, as in troodontids¹². The anterior dentary teeth have bulky crowns, which posteriorly become smaller and more slender.

The hyoid apparatus is rarely preserved in dinosaurs, and *Pelecanimimus* preserves the first hyoid known among Ornithomimosauria. It is V-shaped, with its apex rostrally directed, and is one-third of the skull length.

As is usual in ornithomimosauria, the presacral vertebrae seem to lack pleurocoels⁴, and have platycoelous centra. The neck length is about twice the skull length. The cervical ribs are not fused to the centra, as in *Gallimimus*⁷.

The sternum is not usually preserved in theropods (this has been interpreted either as a preservational bias or as an unossified structure) and was unknown in Ornithomimosauria. Nevertheless, its presence was suspected because of the great distance between coracoids observed in some cases¹⁵. *Pelecanimimus* has a large (and probably paired) sternum, including a rib margin.

As is usual in ornithomimosauria¹⁵, the coracoid has a very conspicuous biceps tubercle and a large posterior process, and

the humerus has a straight shaft. The ulna and radius are tightly adhered distally (Fig. 2b), which could even be a syndesmosis, as in *Struthiomimus altus*¹⁵.

There are five carpals, as in *Struthiomimus*¹⁵. The three metacarpals are close together for nearly all their length. The ratio McI : McII : McIII is 0.81 : 1 : 0.98. The interphalangeal articulations are ginglymous, although articulations with the metacarpals are simpler. Phalanx 1-I is the longest bone of the hand. The length of the 3-III is greater than the combined lengths of phalanges 1-III and 2-III. Unguals are slightly curved, and the flexor tubercles are poorly developed and distally placed. The three digits are subequal in length (as in most derived ornithomimosauria¹⁴) and almost parallel (unlike *Struthiomimus altus*¹⁵, in which the first digit is oriented towards the second and third during flexion). In *Pelecanimimus*, the hand could have worked like a hook, as in *Gallimimus* or *Ornithomimus*¹⁴.

Another surprising feature of *Pelecanimimus* is the preserved impressions that can be clearly observed below the skull, running below the neck and around the right humerus and elbow (Fig. 1). These probably correspond to integumentary structures. They are composed of a primary system of subparallel fibres arranged perpendicular to the bone surface, and a less conspicuous secondary system parallel to it. There is another impression that might correspond to a soft occipital crest. These impressions are the main reason why the counterslabs have not been prepared so far.

The phylogenetic hypothesis (Fig. 3) supports an unexpected approach, involving exaptation¹⁶, which might explain the evolutionary process towards the toothless condition in Ornithomimosauria. Until now, a progressive reduction in the number of teeth has been considered as the most likely explanation¹⁴: the

a	1				22
<i>Allosaurus</i>	00000	00000	00000	00000	00
<i>Albertosaurus</i>	00000	00010	00001	0010-	-0
<i>Deinonychus</i>	00000	00010	00100	00001	00
<i>Garudimimus</i>	10---	11100	1----	-----	--
<i>Gallimimus</i>	10---	11111	11111	1-111	11
<i>Pelecanimimus</i>	01111	10110	11111	11111	11
Troodontidae	01111	11010	10-10	10001	00

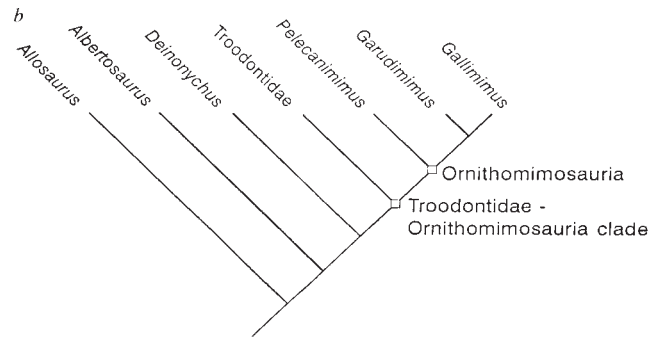


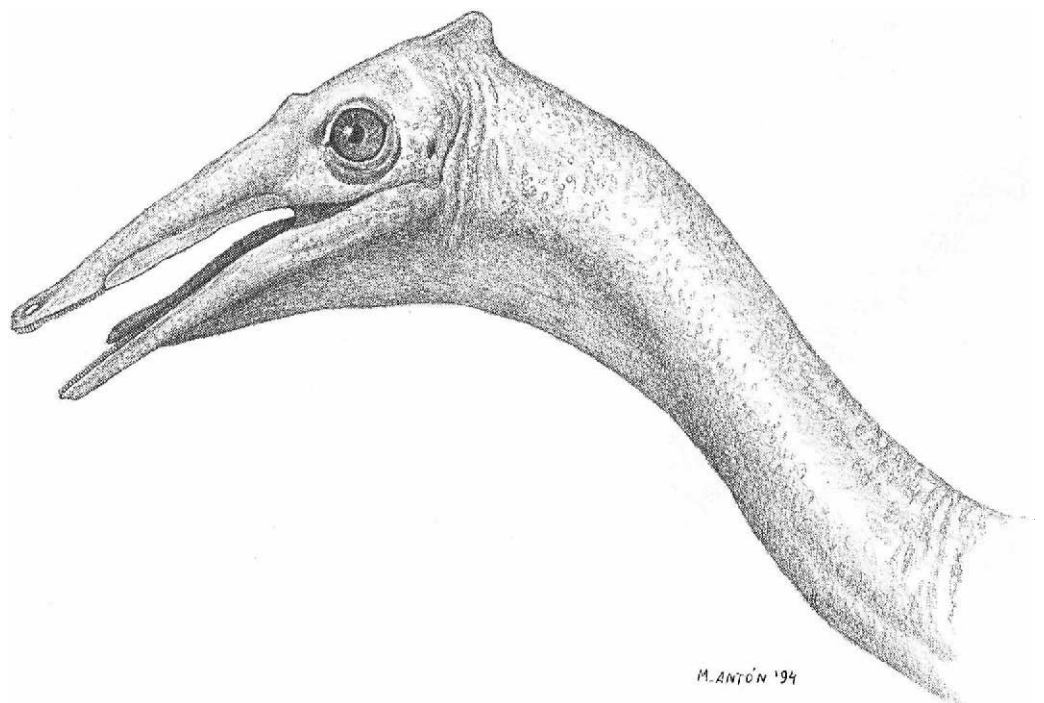
FIG. 3 Phylogenetic analysis. a, Matrix of taxa versus characters. Character states: 0, plesiomorphic state; 1, apomorphic state; -, not preserved/unknown. Derived character states: 1, absence of teeth. The absence of teeth is synapomorphic for all the ornithomimosaurians except *Harpymimus*¹¹ and *Pelecanimimus*. 2, Number of teeth higher than 100. *Allosaurus* has a total of 64–78 teeth⁹, *Deinonychus*, 70 and *Albertosaurus*, 62. Troodontidae have a maximum of 120 teeth¹², and *Pelecanimimus*, has about 220 teeth. 3, Maxillary teeth larger than dentary teeth. 4, Basal constriction in the crown of the teeth. 5, Absence of interdental plates. 6, Skull narrow and shallow, with elongated facial part. 7, Orbit length greater than the antorbital fenestra length. 8, Broad contact between the premaxilla and the nasal. 9, Ventral border of the antorbital fenestra is formed by the maxilla and jugal. 10, Rostral half of the lower jaw ventrally concave. 11, Presence of parasphenoid bulbous capsule. 12, Neck length at least twice the skull length. 13, Coracoid biceps tubercle conspicuous and well developed. 14, Posterior

coracoid process conspicuous and well developed. 15, Humeral shaft straight. 16, Hand/humerus+radius length ratio less than 66%. 17, Ulnar and radial distal ends closely joined, even with a syndesmosis. This character state is unknown in *Gallimimus*⁷, but derived in *Harpymimus*¹¹ and *Struthiomimus*¹⁵. 18, Carpals flat, discoidal. 19, Length of mcl greater than half the length of mcll. 20, Length of the phalanx p3-III greater than that of phalanges p1-III+p2-III. 21, First phalanx of digit I of the hand greater in length than Mcll. 22, Flexor tubercle of unguals not well developed and distally placed. b, Phylogenetic hypothesis. The data matrix was analysed using the implicit enumeration option of ver. 1.5 of the 'Hennig 86' program²². The result is a tree with a consistency index of 0.81 and 28 evolutionary steps. The Troodontidae–Ornithomimosauria clade (previously discussed²³) is defined by seven synapomorphies: characters 3, 4, 5, 6, 11, 14 and 16. *Pelecanimimus* shares seven derived character states with the remaining ornithomimosaurians: 8, 12, 15, 18, 19, 21 and 22.

primitive tetanurine theropods have up to 80 teeth with tall blade-like crowns, and the primitive ornithomimosaurians have only a few small teeth. The phylogenetic hypothesis suggests an alternative evolutionary process based on a functional analysis of increasing numbers of teeth. A high number of teeth with enough interdental space and properly placed denticles (as in troodontids) would be an adaptation for cutting and ripping. On the other hand, an excessive number of teeth with no interdental space (as in *Pelecanimimus*) would be a functional counterpart of the cutting edge of a beak. Thus, increasing the

number of teeth would be an adaptation for cutting and ripping, as long as the space between adjacent teeth was preserved (Troodontidae–Ornithomimosauria clade, Fig. 3b), while it would have the effect of working as a beak if spaces were filled by more teeth (node Ornithomimosauria, Fig. 3b). The adaptation to a cut-and-rip function therefore becomes an exaptation¹⁶ with a slicing effect, eventually leading to the cutting edge seen in most ornithomimosaurians. This tendency is shown by the posterior–anterior replacement of teeth by a cutting border on the maxilla of *Pelecanimimus*.

FIG. 4 Hypothetical reconstruction of *Pelecanimimus* based on cranial and vertebral remains.



The present-day ornithomimosaur European record^{17,18} is doubtful; *Pelecanimimus polyodon* is the first unambiguous evidence of these theropod dinosaurs in Europe. Recent findings seem to indicate that Ornithomimosauria is a more widely distributed group (in space and time) than previously accepted. The reason why the present-day known record is essentially Upper Cretaceous remains unclear. □

Received 22 April; accepted 6 July 1994

- Sanz, J. L. & Bonaparte, J. F. in *Papers in Avian Paleontology Honoring Pierce Brodkorb* (ed. Campbell, K. E. Jr) 39–49 (Nat. Hist. Mus. Los Angeles, Sci. Ser. 36, Los Angeles, 1992).
- Sanz, J. L., Bonaparte, J. F. & Lacasa, A. *Nature* **331**, 433–435 (1988).
- Sanz, J. L. & Buscalioni, A. D. *Palaeontology* **35**, 829–845 (1992).
- Sanz, J. L. et al. *Geobios* **21**, 611–635 (1988).
- Francés, V. & Sanz, J. L. in *La Fauna del pasado en Cuenca. Actas del I Curso de Paleontología* (eds Sanz, J. L. & Buscalioni, A. D.) 125–144 (Instituto Juan de Valdés. Excmo. Ayuntamiento de Cuenca, Cuenca, 1989).
- Vilas, L. et al. *El Cretácico de España* 457–513 (Universidad Complutense de Madrid, Madrid, 1982).
- Osmólska, H., Roniewicz, E. & Barsbold, R. *Palaeont. pol.* **27**, 103–143 (1972).
- Russell, D. A. *Can. J. Earth Sci.* **9**, 375–402 (1972).
- Madsen, J. H. Jr *Bull. Utah Geol. Min. Sur.* **109**, 1–51 (1976).
- Barsbold, R. (in Russian) *Joint Soviet-Mongol. Palaeont. Exp. Trans.* **15**, 28–39 (1981).
- Barsbold, R. & Perle, A. (in Russian) *Paleont. Zh.* **2**, 121–123 (1984).
- Currie, P. J. *J. vert. Paleont.* **7**, 72–81 (1987).
- Russell, D. A. & Dong, Z. *Can. J. Earth Sci.* **30**, 2163–2173 (1993).
- Osmólska, H. & Barsbold, R. in *The Dinosauria* (eds Weishampel, D. B., Dodson, P. & Osmólska, H.) 225–244 (Univ. California, Berkeley, 1990).
- Nicholls, E. L. & Russell, A. P. *Palaeontology* **28**, 643–677 (1985).
- Gould, S. J. & Vrba, E. S. *Paleobiology* **8**, 4–15 (1982).
- Dollo, L. *Mus. Hist. nat. Belgique, Bull.* **2**, 212–214 (1883).
- Seeley, H. G. Q. *J. geol. Soc. Lond.* **39**, 246–253 (1883).
- Maisey, J. G., Rutzky, I., Blum, S. & Elvers, W. in *Santana Fossils. An Illustrated Guide* (ed. Maisey, J. G.) 98–105 (T. F. H. Publications, New York, 1991).
- Ostrom, J. H. *Bull. Peabody Mus. nat. Hist.* **30**, 1–165 (1969).
- Lambe, L. M. *Mem. Geol. Surv. Brch Can.* **100**, 1–84 (1917).
- Farris, J. *Hennig 86 references. Documentation for version 1.5* (1988).
- Hoitz, T. R. Jr *J. Paleont.* (in the press).

ACKNOWLEDGEMENTS. We thank R. Barsbold, T. R. Holtz Jr, J. H. Madsen Jr and H. Osmólska for suggestions; A. Díaz Romeral, A. Fregenal and N. Meléndez for finding some parts of the specimen; G. F. Kurtz for photography and M. Antón for the drawing. This work was supported by Junta de Comunidades de Castilla-La Mancha, DYGCYT (Promoción General del Concimiento) and the European Community (Human Capital and Mobility Program).

Active anaphylaxis in IgE-deficient mice

Hans C. Oettgen*, Thomas R. Martin††, Anthony Wynshaw-Boris*, Chuxia Deng*, Jeffrey M. Drazen†† & Philip Leder*

* Department of Genetics, Harvard Medical School, Howard Hughes Medical Institute, 200 Longwood Avenue, Boston, Massachusetts 02115, USA

† Department of Pediatrics, Ina Sue Perlmutter Laboratory, The Children's Hospital and Harvard Medical School, Boston, Massachusetts 02115, USA

‡ Department of Medicine, Brigham and Women's Hospital and Harvard Medical School, Boston, Massachusetts 02115, USA

THE IgE-triggered release of mast cell mediators in response to antigen is thought to be the primary event in immediate hypersensitivity reactions such as systemic anaphylaxis¹. Although mast cells and basophils can be activated *in vitro* by non-IgE stimuli^{2–5}, it is not known whether these triggers lead to physiological changes *in vivo*. To investigate this possibility, we generated mice with a homozygous null mutation of the *Cε* gene. Such mice make no IgE, but produce other immunoglobulin isotypes normally. We report that despite the IgE deficiency, sensitized mutant mice become anaphylactic on antigen challenge and display tachycardia and pulmonary function changes similar to those seen in wild-type animals. These responses are accompanied by vascular leak, sharply elevated plasma histamine and rapid death. IgE-independent anaphylaxis does not depend on complement activation, but, as indicated in studies using genetically immunodeficient *RAG-2*⁻

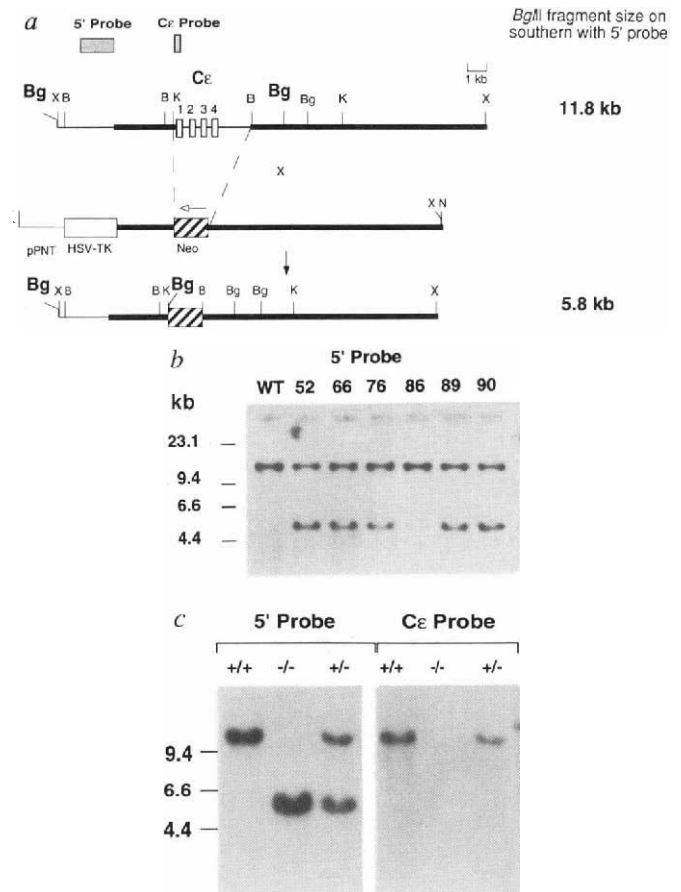


FIG. 1 Generation of mice with complete deletion of the *Cε* exons. **a**, The targeting vector. The replacement-type targeting construct contained 3.2 kb of genomic DNA upstream of the *Cε* exons and 10 kb of downstream homologous sequence (thick lines). The positions of a neomycin resistance gene (Neo, hatched box) replacing the *Cε* exons as well as a herpes simplex virus thymidine kinase gene (HSV-TK, white box) for positive/negative selection are indicated. *Bgl*III sites giving rise to a restriction fragment length polymorphism between the wild-type locus and the targeted allele using a 5' flanking probe are shown (Bg, *Bgl*III; X, *Xho*I; B, *Bam*HI; K, *Kpn*I). **b**, Identification of targeted ES clones. *Bgl*III-digested genomic DNA from ES clones was analysed by Southern blotting using a 5' flanking probe. A 5.8 kb band diagnostic of homologous recombination was present in the six clones (of 100 screened) shown. The first lane contains wild-type DNA. **c**, Southern analysis of tail DNA from the offspring of chimaeric mice generated by blastocyst injection with clone-89 ES cells. Three genotypes, +/+, -/- and +/- were detected. Rehybridization of the same DNAs with a *Cε* exon-specific probe confirmed that this sequence was absent from the genomic DNA of -/- animals.

METHODS. 129/Sv genomic clones containing the *Cε* exons and flanking sequences were isolated from a λ FIX II library (Stratagene) using a *Cε*1 probe generated by PCR. The vector pPNT, kindly provided by V. Tybulewicz, was used to prepare the targeting construct²⁷. pPNT contains the neomycin resistance gene (neo) under the control of the phosphoglycerate kinase promoter (PGK). The linearized targeting construct (25 μ g) was introduced into 10^7 J1 ES cells (kindly provided by En Li and R. Jaenisch) by electroporation²⁸. Selection was initiated at 24 h using G418 and the gancyclovir analogue, FIAU. Clones were recovered at 8 days, aliquots frozen and DNA prepared for Southern analysis using the 5' flanking probe. Clone-89 was injected into blastocysts and the resultant chimaeric male pups mated with black Swiss females (Taconic). The offspring of these matings included animals heterozygous for the *Cε* disruption. These were then bred to homozygosity.

and *SCID* mice, does require a functional immune system. Such results clearly demonstrate that non-IgE pathways for hypersensitivity reactions exist in mice.

A null mutation in the IgE gene was prepared by deleting exons *Cε*1–4 encoding the constant region domains of the ϵ -